軟弱砂岩力學行為與微觀機制研究 (II)
The Study of The Mechanical Behavior And The Microscopic Mechanism of Weak Sandstones (II)

計畫編號：NSC 89-2211-E-002-152

執行期限：89/8/1-90/7/31

主持人：鄭富書　台灣大學土木工程學系 副教授

☑ 出席國際學術會議心得報告及發表之論文各一份

一、摘要

中文摘要(關鍵詞：軟弱砂岩，剪脹，組成模式)

所謂「剪脹」，是指材料在尖峰應力前，受純剪應力而產生膨脹的現象，與一般彈性等向性材料受純剪時，體積應變為零的行為有異。大地材料具有剪脹的特性，軟弱砂岩尤其顯著，其對工程的影響相當深遠，因此有必要發展一剪脹模式來進行工程分析。

本研究參考前人文獻，基於等向性材料受剪後產生「異向性破壞」，造成剪力模數弱化的觀念切入，認為主應力空間下，某材料受一應力狀態，最大主應力導致材料之異向性。

觀察三軸試驗中岩石的應力應變行為，透過合理的簡化，期能發展出簡易的模式來描述大地材料的剪脹行為。本模式中利用三個參數E、G及G'來描述，其中E為楊氏模數，G為剪力模數，G'為環向剪力模數。此三個參數均可以藉由試驗室中，不同圍壓下，對試體進行純剪應力路徑試驗而得。

最後，運用有限元素法，先利用單元素比對本模式在不同應力路徑下之行為，再將本模式分別代入隧道案例、基礎案例、邊坡案例分析，以探討本模式在工程分析上的適用性。

英文摘要(Keyword: soft sandstone, shear dilation, constitutive model)

The "Shear dilation" means the dilation behavior of the geo-materials under the shear stress state. As everybody knows, the linear elastic isotropic material will only change its shape rather than volume when it is subjected to shear stress. However, some other geo-materials such as soft rock and dense sand behave in different ways and deform a lot when subjected to shear stress. This important characteristic of these materials far affects the deformation of civil construction. It is necessary for us to develop a simple and reasonable constitutive model to describe the deformation behavior.

The research intends to characterize the deformation behavior and proposes a constitutive model with three parameters E、G、G'. The model is on the basis of the concept that anisotropy is caused by shear stress. It is assumed that in the principal stress space the shear stress weakens the shear modulus G so that shear dilation may occur. All the parameters can be got easily from

tri-axial tests. A procedure is also introduced to show how to get these parameters.

In order to verify the accuracy of this model, we compare the laboratory tri-axial test data with the predicted values of the model. The results show this model is reliable. To take better control of the deformation we concern, we use the shear dilation model to analyze some civil engineering problems by finite element method.

二、計畫緣由與目的

台灣地形多山地，且地質構造複雜，西部麓山帶地區大多為第三紀沉積地層，岩石膠結及壓密程度不佳，大部分強度不高且易風化，造成軟弱、破碎岩石特別多。隨著人口增加，都市發展，各種大地工程難免會遇到此類不利施工的岩石，例如北二高沿線的木柵隧道與中和隧道在通過木山層砂岩後，即發生嚴重的擠壓變形問題，導致機具損害、工程延誤。

軟弱岩石在受力達尖峰應力前，具有「剪脹」的特性，也就是受剪應力作用下，產生膨脹的現象。一般彈性等向性材料，其承受剪應力時，體積並不會發生變化，也就是剪應力與體積應變並無偶合的作用。

軟弱岩石此種剪脹的特性，對工程分析而言相當重要，若忽略掉此效應，將低估岩石的變形性。因此，本年計劃之研究目的即在於分析過去對於軟岩所進行一系列的純剪實驗結果，並提出一套合理簡單的模式，以供進行分析時，更能掌握岩石的變形性。

三、剪脹模式

在彈性等向性材料中，材料的組成律模式可以用主應力與主應變的增量形式表示如下：

$$\begin{Bmatrix}\Delta\varepsilon_1\\ \Delta\varepsilon_2\\ \Delta\varepsilon_3\end{Bmatrix}=\frac{1}{E}\begin{bmatrix}1 & -\frac{E-2G}{2G} & -\frac{E-2G}{2G}\\ -\frac{E-2G}{2G} & 1 & -\frac{E-2G}{2G}\\ -\frac{E-2G}{2G} & -\frac{E-2G}{2G} & 1\end{bmatrix}\begin{Bmatrix}\Delta\sigma_1\\ \Delta\sigma_2\\ \Delta\sigma_3\end{Bmatrix} \quad (1)$$

式中：E 為材料之楊氏模數；G 為剪力模數。

本研究所討論之剪力模數 G，均指切線剪力模數，從三軸試驗數據所求。

參考 Aristorenas (1992)之頁岩組成律模式與 Chang(1995)之模式，某材料受一應力狀態，在主應力空間下，最大主應力導致異向性，因而產生非等向性破壞。本剪脹模式假設當材料受到剪應力作用而產生異向性後，造成 G 的弱化，且異向性方向為最大主應力方向，材料的組成律式可改寫成如下之形式：

$$\begin{Bmatrix}\Delta\varepsilon_1\\ \Delta\varepsilon_2\\ \Delta\varepsilon_3\end{Bmatrix}=\frac{1}{E}\begin{bmatrix}1 & -\frac{E-2G}{2G} & -\frac{E-2G}{2G}\\ -\frac{E-2G}{2G} & 1 & -\frac{E-2G'}{2G'}\\ -\frac{E-2G}{2G} & -\frac{E-2G'}{2G'} & 1\end{bmatrix}\begin{Bmatrix}\Delta\sigma_1\\ \Delta\sigma_2\\ \Delta\sigma_3\end{Bmatrix} \quad (2)$$

定義 G 為軸向對環向的剪力模數，G'為環向對軸向的剪力模數，當材料未受到剪應力時，G 和 G'是相等的，材料表現出等向性材料之特性，若材料承受剪應力時，G 和 G'開始出現差異。本研究即以此模式，描述大

地材料受剪膨脹的行為。

依照上述觀念及實驗結果，本模式中之E、G、G'可表示如下：

$$G=\left(c\frac{I_1}{3}+d\right)\left(1-(\frac{\sqrt{J_2}}{\sqrt{J_{2,f}}})^2\right) \qquad (3)$$

$$G'=\left(c\frac{I_1}{3}+d\right)\left(1-(e\frac{\sqrt{J_2}}{\sqrt{J_{2,f}}})^2\right) \qquad (4)$$

$$E=2(1+\nu)G$$
$$=2(1+\nu)\left(c\frac{I_1}{3}+d\right)\left(1-(\frac{\sqrt{J_2}}{\sqrt{J_{2,f}}})^2\right) \qquad (5)$$

其中，$c=\frac{3a(1-2\nu)}{2(1+\nu)}$、$d=\frac{3b(1-2\nu)}{2(1+\nu)}$，而破壞準則採用 Drucker-Prager 破壞準則。表示如下：

$$\sqrt{J_2}_{,f}=\alpha I_1+k\text{。} \qquad (6)$$

四、剪脹模式之驗証

為了驗証本剪脹模式之正確性，研究中選擇與蔡立盛 (2000) 對木山層砂岩所做的不同應力之三軸試驗結果比對。

本模式主要目的在模擬剪脹的行為，因此模式所得到的變形，必須能符合材料受到各種不同應力時的變形。

由於本模式的應力增量均定義在主應力空間中，而在三軸試驗中，所加的軸壓和圍壓均為主應力，因此我們可以輕易地決定主應力的大小。將試驗中所施加的應力路徑，代到本剪脹模式中，若此模式正確，則試驗所得的變形與模式所得之變形應該要一致。

在應力路徑的選擇上，選擇傳統三軸應力路徑、純剪應力路徑與實驗數據做比對。

以傳統三軸應力路徑為例，將此試驗之應力歷程代入本模式中，我們可以觀察到E、G、G'在整個應力路徑的變化情形如圖一。在加圍壓段，E、G、G'呈線性變化，G＝G'；在軸差壓階段，E、G、G'均開始弱化，但此階段之初，體積應力增加造成的效應大於剪應力的弱化效果，因此E、G、G'均為先變大後再減小，且G和G'開始出現差異而產生剪脹效應。

在此應力路徑下，材料之變形與試驗數據的結果比較如圖二。在加圍壓至20 MPa的階段，模式與試驗相當吻合，代表本模式可以描述材料未受剪時，隨圍壓增大而變硬時之變形行為；在加軸差壓階段，初始時模式之變形結果與試驗尚相當一致，然隨著軸差壓增大，兩者間開始有些許差異，當材料接近破壞時，試驗試體出現體積膨脹的現象，本模式亦表現受剪膨脹的行為，此時材料之變形在最後又趨向相同。

本模式主要為模擬材料受剪後之膨脹行為，圖二中雖與試驗試體之變形行為有所差異，然整體之體積變化仍屬一致。

五、案例分析

本研究將剪脹模式代入隧道及基

礎案例分析。

5.1 隧道案例分析

茲以國內某隧道案例為例，以平面應變數值模式為基礎，將數值分析結果與現地監測資料之變形趨勢作一比較，以探討本研究剪脹模式、彈性模式與彈塑性模式與，隧道變形行為之異同。本研究隧道案例覆土深度約為 70 公尺，隧道斷面寬為 16 公尺，高為 11.4 公尺。

本案例中，將分析流程分為三個步驟，第一個步驟為施加隧道模型自重，第二個步驟為左隧道上半斷面移除，第三個步驟為左隧道下半斷面移除。

本研究之剪脹模式中，剪力模數 G 值隨剪應力之增大而遞減。由上述討論，隧道於大地應力施加時，因無剪應力存在，剪力模數並不弱化。隧道開挖後，其周圍之岩體，剪應力會不斷增加，而本模式受剪應力後，造成岩體剪力模數弱化，因此形成一圈弱化區，與只加大地應力時的剪力模數分佈比對，結果如圖三。

彈性模式、彈塑性模式和剪脹模式中，繪製頂拱、仰拱和側壁變位之歷時圖，如圖四所示，由圖可知剪脹模式分析之變形量，均比彈性模式和彈塑性模式大。由圖五之應力路徑知隧道開挖時，所受應力以剪應力為主，而本模式岩體受剪後有體積膨脹，而彈性模式受剪時無體積應變，故本模式之變形均比彈性模式大。

5.2 基礎案例分析

本案例考慮一基底粗糙之長條形淺基礎，寬為 8 m，置於均質、等向性、為無限土壤表面上。本案例為平面應變，且左右對稱，基礎中線為對稱軸，故建立模型時，僅取右半部建立模型，以進行分析，模型網格如圖六。模型的尺寸為 24.4 公尺 x 150 公尺，基礎寬之半為 4 公尺，模型 150 公尺的寬度已不致對分析結果產生影響。

由分析結果中顯示，其應力路徑如圖七，由圖可知基礎分析之應力路徑與傳統三軸應力路徑相似，體積應力與剪應力均增加，基礎角隅下之元素受力較基礎中央下之元素大，且先達破壞。基礎承受荷重之後，其剪應力分佈圖如圖八，基礎下方剪應力會增加，形成一弧狀之剪力帶。

將本模式分析之沉陷量與彈性模式、彈塑性模式、Harr (1996) 及 Janbu (1956)等理論公式比對，如圖九。本模式分析結果，沉陷量在低荷重時，與彈性及彈塑性模式相近，然隨著荷重持續增加，沉陷量逐漸大於彈性及彈塑性模式之分析結果，且最後有一明顯之轉折點而達降伏。若與理論模式相比，則與 Harr 所提出之理論較接近。整體而言，以本模式之沉陷量為最大。

各模式之危險因子如圖十所示。彈性模式、彈塑性模式和本模式之危險因子均以基礎角隅為最大，且本模式危險因子大於 1 之區域較大，代表以本模式分析較彈性模式及彈塑性模式保守。

六、結論

本研究之結論如下：

(1) 本模式在未受剪應力時，具等向性材料之性質，受剪應力後，即表現出異向性之性質，此異向性與最大主應力方向相同。

(2) G 和 G'值均為體積應力和剪應力的函數，材料受剪後，G 和 G'均會弱化而變小，然弱化的程度不同，受剪後若 $G > G'$，則呈現剪縮的現象，若受剪後 $G < G'$，則材料表現剪脹行為。

(3) 本模式在不同應力路徑下所預測之材料變形，與試驗室所得之試驗結果大致相同，因此可以合理地描述剪脹行為。

(4) 隧道案例分析時，藉由危險因子，可判斷本模式分析之危險區與彈性模式和彈塑性模式相似，然危險因子值較大。而隧道之變形量，無論頂拱、仰拱和側壁，均較彈性及彈塑性模式為大，故使用本模式分析較保守。

(5) 基礎案例分析時，本模式之破壞區較彈性模式與彈塑性模式大，沉陷量亦是本模式較大。若荷重-沉陷量之關係圖中，本模式有一明顯之轉折點，可得到極限承載力。

參考文獻

[1] 賈勇華 (1996)，軟弱岩石隧道數值分析模式研究，國立台灣大學碩士論文，台北。

[2] 蔡立盛 (2000)，粗顆粒砂岩三軸實驗技術改善-以木山層砂岩為例，國立台灣大學碩士論文，台北。

[3] 陳鴻仁 (2000)，大地材料剪脹行為模式初探，國立台灣大學碩士論文，台北。

[4] Aristorenas, G.V., 1992, Time Dependent Behavior of Tunnels Excavated In Shale Ph. D. Thesis, Massachusetts Institute of Technology

[5] Sakurai, S , 1998, "Determination of Strength Parameters of Rocks by a Back Analysis of Measured Displacements," Regional Symposium on Sedimentary Rock Engineering Nov. 20-22, Taipei, Taiwan, Roc

[6] Zhao, Y.H., 1998, "Crack Pattern Evolution and a Fractal Damage Constitutive Model for Rock," Int. J. RockMech. Sci. Vol. 35, No. 3, pp. 349-366

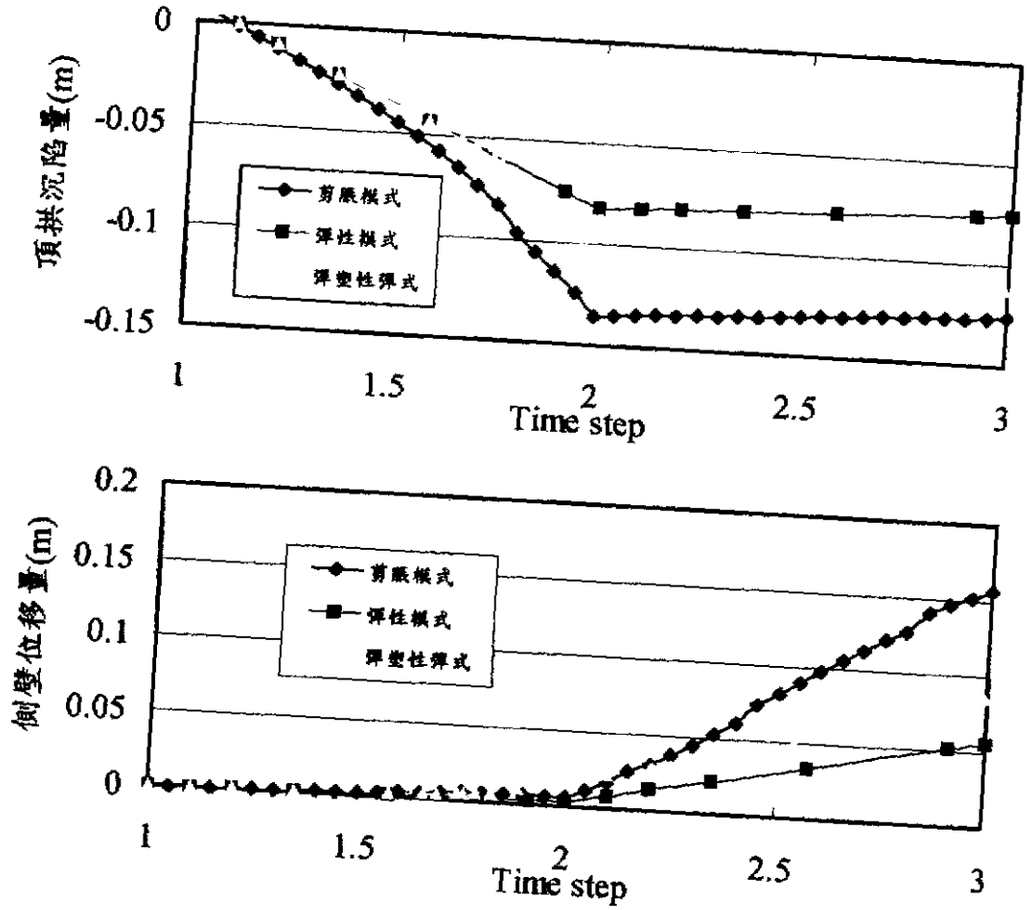

圖四　頂拱和側壁變位之歷時圖

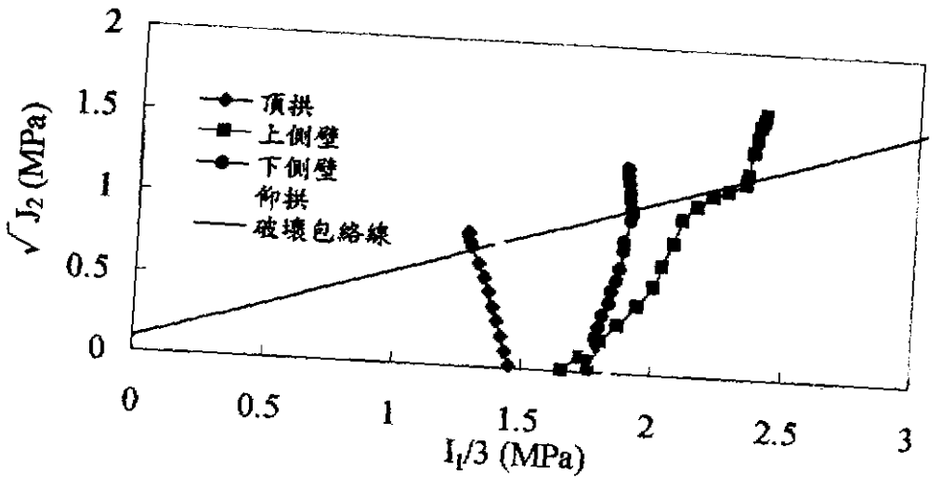

圖五 隧道案例頂拱、側壁、仰拱之應力路徑

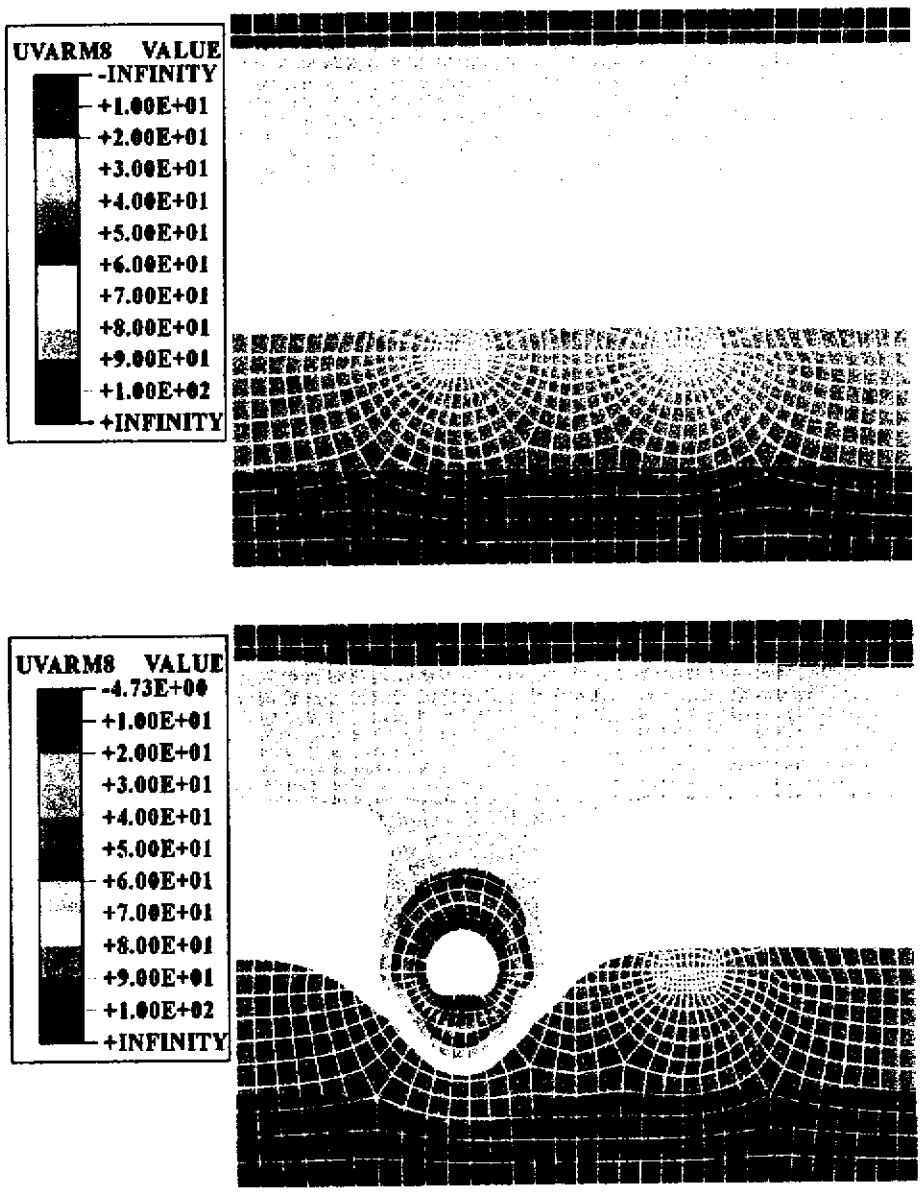

圖三　開挖前後之剪力模數分佈圖

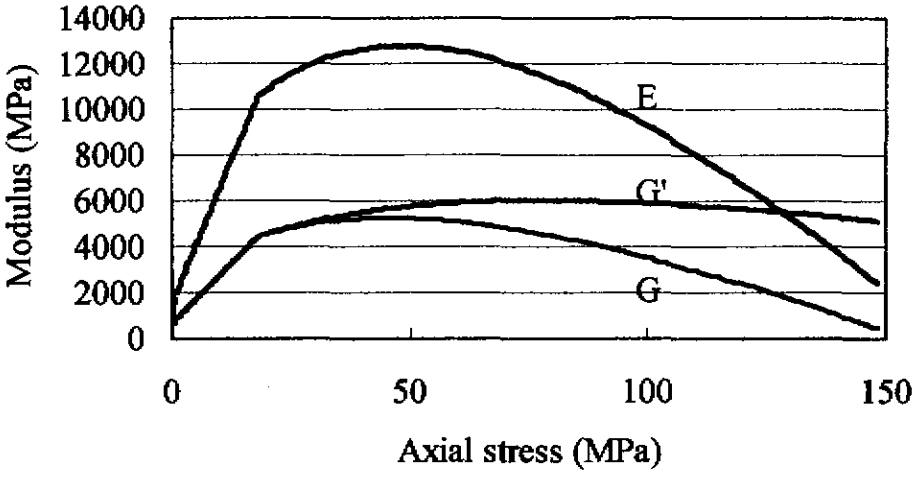

圖一　傳統三軸應力路徑時E、G、G'的變化情形

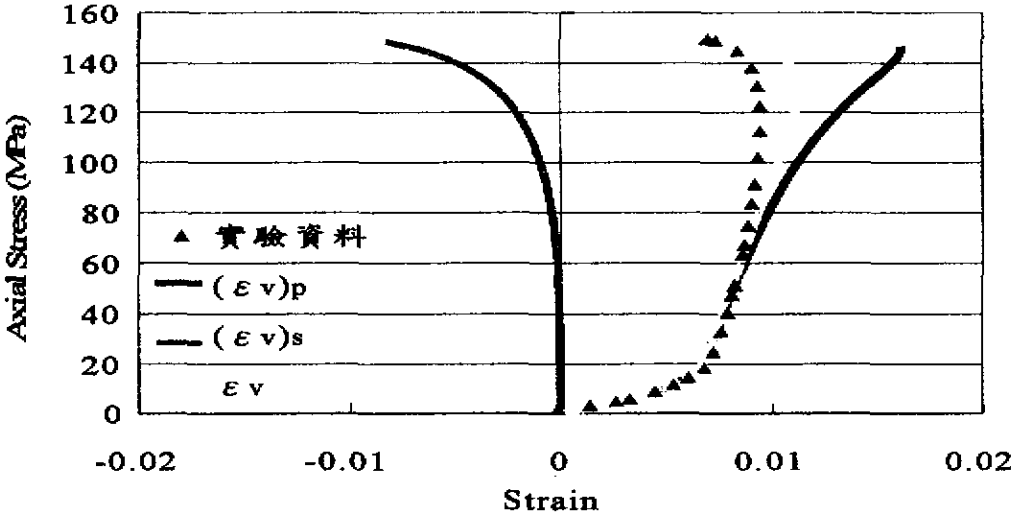

圖二　傳統三軸應力路徑時，剪脹模式應變與試驗數據比較

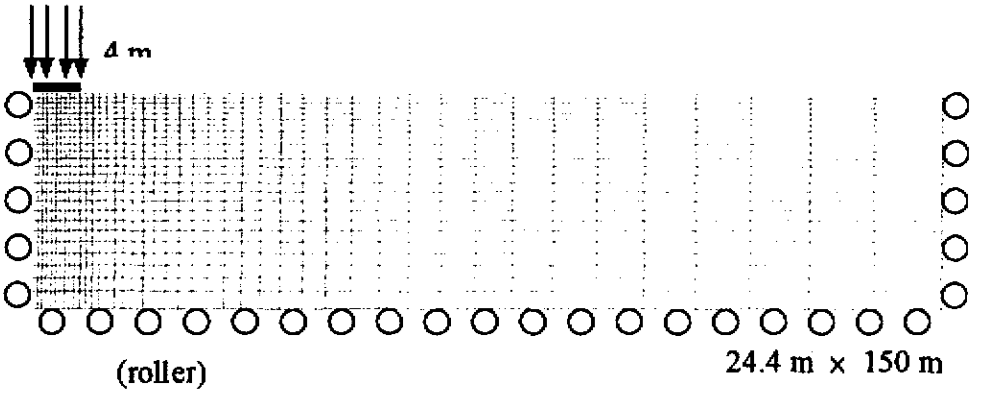

圖六 基礎案例之分析網格圖

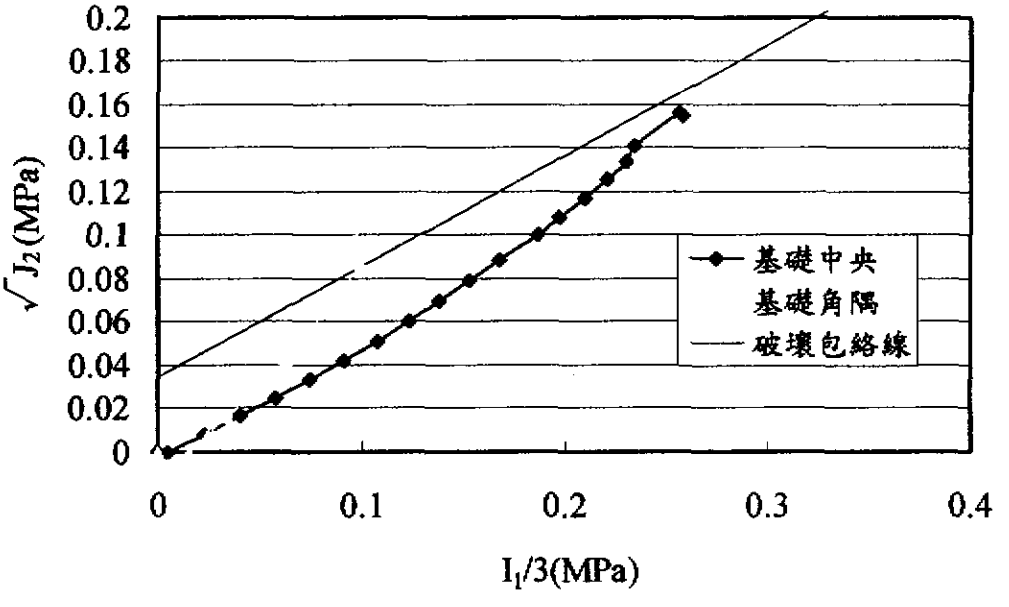

圖七 基礎承受荷載時之應力路徑

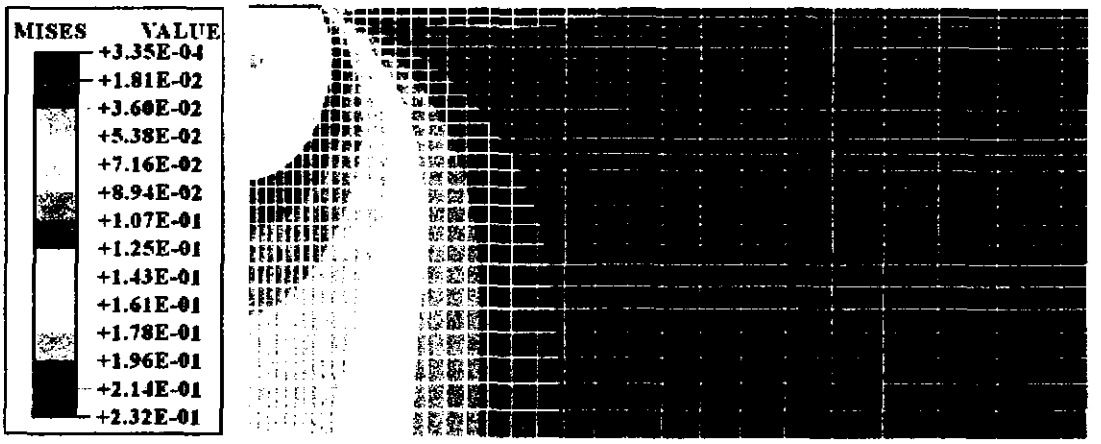

圖八 基礎承受荷載時之剪應力分佈圖

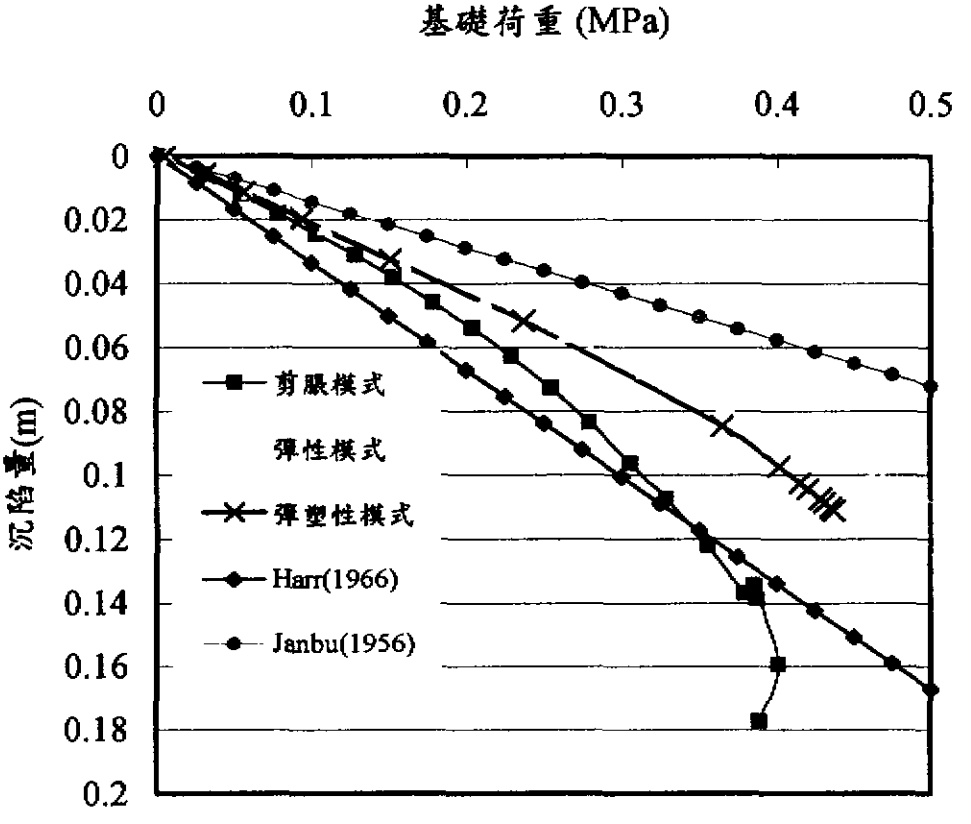

圖九 不同模式下基礎荷重與沉陷量之關係圖

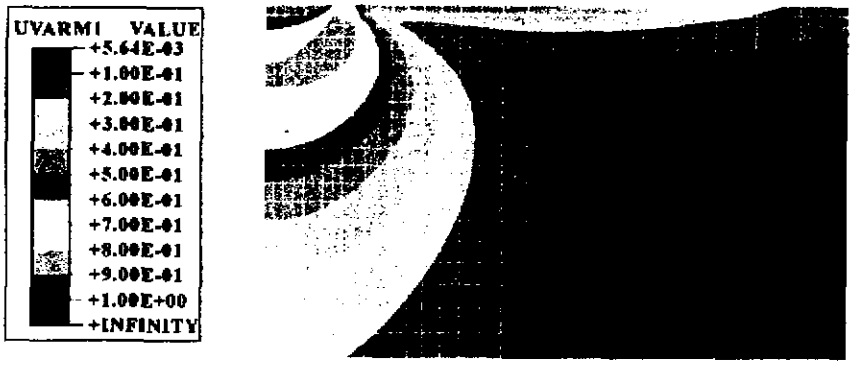

彈性模式

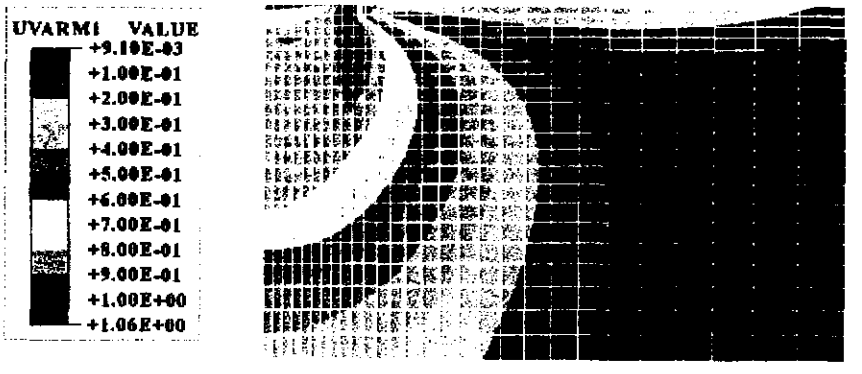

彈塑性模式

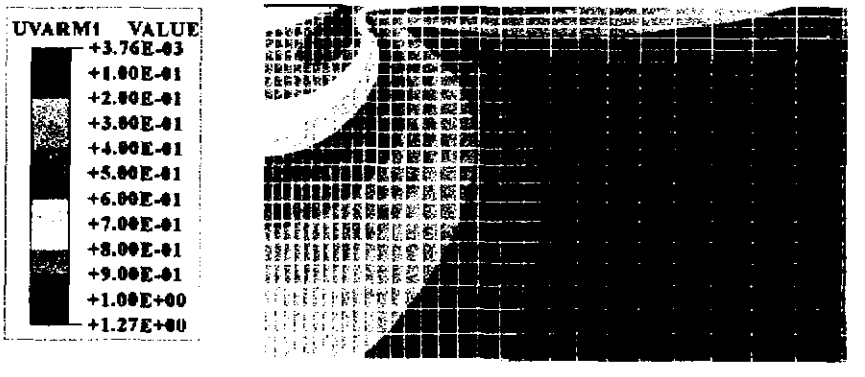

剪脹模式

圖十 基礎承受荷載後各模式之危險因子圖

行政院國家科學委員會補助國內專家學者出席國際學術會議報告

90 年 2 月 5 日

報告人姓名	鄭富書	服務機構及職稱	國立臺灣大學 副教授
會議時間 會議地點	90 年 1 月 7 日至 13 日 美國 亞利桑那州 Tucson 市	計畫編號	NSC89-2211-E002-152
會議名稱	(中文) 第十屆國際計算方法及大地力學會議 (英文) The 10th International Conference on Computer Methods and Advances in Geomechanics		
發展論文題目	Buckle folding of elastic strata		
會議地點	Tucson, Arizona, United States.		

一、 研討會概述

大地工程數值方法與應用國際研討會，是關於數值分析方法應用在大地工程領域方面一個相當具有規模的國際研討會。會議之目的為集結各國大地工程數值分析研究之科學家、工程師、及相關從業人仕，能夠在一個正式的場合溝通交換有關利用數值分析由大地材料基本力學性質到工程實務應用各層面研究的經驗與想法，以促進大地工程領域在數值資訊技術上的提昇與進步。

此研討會每兩年舉辦一次，前一次會議於 99 年在大陸武漢市舉行，今年則已邁入第十屆。本屆研討會由美國亞歷桑那大學主辦，於 2001 年 1 月 7 日至 12 日在美國亞歷桑那州土桑市（Tucson）舉辦。這一次會議的主題是「由基礎到應用」（Fundamentals Through Applications），企圖從最基礎的力學性質、材料組成律的研究，到大地工程實務上的應用，都能夠充份發揮數值分析的優勢，讓數值分析這項資訊技術能夠幫助提昇大地工程及地質力學領域相關研究的廣度和深度，而能夠在方法論上去解決各種特殊的問題與挑戰。

此次研討會收錄了 320 篇左右論文，約有 280 篇論文在於五天的研討會中分四個會場進行發表或討論。研討會中發表的論文內容涵括了以下幾個部份：基礎理論(theory)、數值方法(computational methods)、組成律與組成模式(constitutive laws, constitutive models)、動態分析(dynamics, earthquake analysis, liquefaction)、滲流與壓密(seepage, consolidation)、節理及介面(joints, interfaces)、破裂力學(microcrackin,

localization, fracture, nano-micro-macro correlation)、試驗(testing, validations, parameter determination)、專家系統(neural networks, expert systems, reliability, optimization)、地質模擬(geological simulation, hydraulic fracturing, petroleum geomechanics)、基礎工程(foundation, footings, piles)、邊坡工程(slopes, dams, walls, landslides)、地下工程(tunnels, underground work, mining)、地質環境工程(geoenvironmental engineering)其它各種工程應用(applications)及教育推展(education)。

本人在會議中所發表的論文題目為"Buckle folding of elastic strata"，探討岩盤褶皺作用、post-buckle 行為及其主控因素，並提出傳統正弦波形以外之另二種褶皺形態(雙頻波形及振幅衰減現象)。本文共同作者為 C. Y. Lu 及 N. G. Chang。

二、 與會心得

隨著資訊技術一日千里的發展，數值方法已逐漸成為方便而重要的工具，在各個不同的議題上都已經有相當顯著的研究成果。數值方法的發展，已可以在個人電腦平台進行大量資料運算和處理的困擾，讓重覆性演算工作不再成為研究的負擔，同時也因此開展了更大的研究空間和視野。因此數值分析可在研究歷程中扮演重要之工具角色，可以進行數值之「實驗」，容易控制邊界條件、模型組態及材料性質與行為，實為物理實驗之外之另一有效工具。

在大地工程領域的研究上，由於大地材料之行為豐富，包括彈性、塑性、非線性、依時性、應力路徑相關、異向性、組成的異質性及其分佈上的不確定性…等，再加上大地工程大變形；使得數值分析應用於大地工程更具挑戰。綜觀本屆發表研究成果內容，有關大地材料性質之模擬與開發仍佔 1/3 左右，其發展仍屬蓬勃。

三、 攜回資料

1. 大會議程
2. IACMAG10 會議論文集二冊
3. International Journal of Geomechanics

4. Pellant C. and R. Phillips (1990): Rocks, Minerals & Fossils of the World, Little & Brown, Boston.
5. Parker, S.P. (1994): Dictionary of Geology & Minerals, McGraw-Hill, New York.
6. Hammond World Atlas Corp. (2000): New Century World Atlas.
7. Harrison, J.P. and Hudson, J.A. (2000): Engineering Rock Mechanics, Pergamon, London.
8. Press, F. and R. Siever (2000): Understanding the Earth, 3rd ed., Freeman, New York.
9. Arduini, P. and G. Teruzzi (1986): Fossils, Fireside, New York.
10. Brocardo, G. (1994): Minerals & Gemstones of the World. Davis & Charles, Devon.
11. 岩石標本數件(三葉蟲、化石木、Obsidian、自然銅礦)

(以上書籍、岩石標本均以私人款項購買)

Computer Methods and Advances in Geomechanics, Desai et al. (eds) © 2001 Balkema, Rotterdam, ISBN 90 5809 183 X

Buckle folding of elastic strata

F.S.Jeng & N.G.Chang
Department of Civil Engineering, National Taiwan University, Taipei, Taiwan
C.Y.Lu
Department of Geology, National Taiwan University, Taipei, Taiwan

ABSTRACT: This paper presents a general solution of an elastic layer embedded in soft material, which has been partly discussed. This solution is then compared to finite-element simulation using a proposed perturbation method, which can exclude the effect of initial geometry imperfection. The numerical simulation reveals both of the waveform and the post-buckle behavior of elastic competent strata. It is observed that, waveform comprised of two frequencies may occur as the exerted force F is greater than a critical force, F_{cr}. When $F < F_{cr}$, the amplitude will decay as the distance to the perturbed end increases. Meanwhile, the mechanism of two-ordered fold and poly-harmonic fold are discussed in this paper.

1 INTRODUCTION

While folding under high confining stress and high temperature condition, the stratum (e.g. metamorphic rocks) exhibits viscous behavior and hence, the folding behavior is frequently analyzed using viscous theories (Biot, 1961; Fletcher, 1977; Mühlhaus *et al.*. 1998; Hunt *et al.*, 1996). However, folding of sedimentary rocks, namely under low confining stress and temperature condition, can still often be observed. Therefore, analyses based on the elastic behavior of stratum were accordingly conducted (Currie *et al.*, 1962; Hunt *et al.*, 1993). Numerical analyses to reveal the mechanism of non-viscous folding have also been conducted (Cobbold, 1977; Lan & Hudleston, 1991).

The simulation of folding using numerical method involves shortening of the strata, a perturbation to induce folding and a subsequent shortening to further deform the folds. The perturbation is induced by the "initial geometric imperfection" of the layer (Zhang *et al.*, 1996), which often is a consequence of natural sedimentary process. However, this initial imperfection can sometimes influence the characteristics (e.g. wavelength) of the yielded fold, which unfortunately interferes the interpretation of the folding mechanism (Mancktelow, 1999). Therefore, it is wished that the effect of the mechanical characteristics of the strata (e.g. stiffness and thickness) upon the folding behavior could be isolated from the effect of the initial perturbation geometry.

Another perturbation method, which excludes the effect of initial geometry imperfection, is therefore proposed in this paper. The layer is first shortened, followed by employing a small rotation at the boundary to apply a moment to the layer to induce folding. The result indicates that this technique yields folds corresponding only to the characteristics of the strata without any influence from the initial perturbation geometry.

To explore the mechanism associated with folding of an elastic layer, this paper presents a complete closed form solution of a layer embedded in soft material, which has been partly discussed (Karman & Biot, 1940; Currie *et al.*. 1962). The solution is then compared to the results of finite-element simulation. The mechanism of poly-harmonic fold is also discussed in this paper.

2 STRATUM SURROUNDED BY SOFT MATRIX – ELASTIC THEORY

2.1 Stratum surround by spring

First, considering a stratum embedded in soft matrix comprised of elastic springs, the governing equation is (Karman & Biot, 1940):

$$Y''''(X)+\frac{F}{EI}Y''(X)+\frac{K}{EI}Y(X)=0 \qquad (1)$$

where: Y, E and I are the vertical displacement, Young's modulus and moment of inertial of the stratum, respectively; K is the stiffness of the spring; and F is the horizontal force required to buckle the stratum, namely to produce a fold.

Solving Eqn. 1, the characteristic value λ can be determined by the F, E, I and K as:

$$\lambda = \pm\sqrt{\frac{-F \pm \sqrt{F^2 - 4EIK}}{2EI}} \tag{2}$$

The solution of Eqn. 1 depends on the relative magnitude of the exerted force F and the rigidity of the stratum and spring ($\sqrt{4EIK}$). When $F \geq \sqrt{4EIK}$, the required force F for yielding a fold with wavelength (l) can be related as:

$$F = \frac{4\pi^2}{l^2}EI + \frac{Kl^2}{4\pi^2} \tag{3}$$

Fig. 1 illustrated the relation of F with l when $F \geq \sqrt{4EIK}$, based on Eqn. 3.

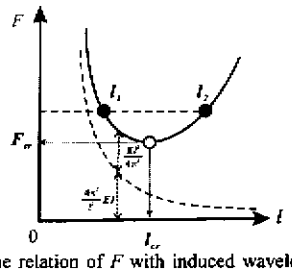

Figure 1 The relation of F with induced wavelength l *when* $F \geq \sqrt{4EIK}$ (after Karman & Biot, 1940).

As illustrated by Fig. 1, when $F \geq \sqrt{4EIK}$, a critical force (F_{cr}) exists with a corresponding wavelength l_{cr}, which are:

$$F_{cr} = \sqrt{4KEI} \tag{4}$$

$$l_{cr} = 2\pi\sqrt[4]{\frac{EI}{K}} \tag{5}$$

For $F > F_{cr}$, the solution of Eqn. 1 is a wave comprised of two frequencies:

$$Y = a\sin mX + b\cos mX + c\sin nX + d\cos nX \tag{6}$$

where m and n are:

$$m = \sqrt{\frac{-F + \sqrt{F^2 - 4EIK}}{2EI}} \tag{7a}$$

$$n = \sqrt{\frac{-F - \sqrt{F^2 - 4EIK}}{2EI}} \tag{7b}$$

The wavelengths corresponding to m and n are (Fig. 1):

$$l_1 = \frac{2\pi}{m} \text{ ; and } l_2 = \frac{2\pi}{n} \tag{8}$$

Yet, when $F < F_{cr}$, folding of the stratum is still possible, which is not well discussed so far. When $F < F_{cr}$, solution of Eqn. 1 has the following form:

$$Y = e^{-nx}(a\cos nx + b\sin nx) \tag{9}$$

where m and n are determined by the exerted force F and the property of material (E, I and K) as:

$$m = \sqrt{\frac{-F + \sqrt{4EIK}}{4EI}} \tag{10a}$$

$$n = \sqrt{\frac{F + \sqrt{4EIK}}{4EI}} \tag{10b}$$

Based on Eqn. 9, the fold has only one frequency and the amplitude tends to decay as x (the distance from the perturbed end) increases.

The relation of F with the wavelength l can be expressed as (Fig. 2):

$$F = \frac{16\pi^2 EI}{l^2} - \sqrt{4EIK} \tag{11}$$

Eqn. 11, indicate that: (1) folding is possible even when the exerted force is close to zero; (2) the less the F, the greater the wavelength l and the severer the decay of amplitude as well; and (3) when F approaches zero, a maximum wavelength (l_3) exists, which can be expressed as:

$$l_3 = \frac{4\pi\sqrt{EI}}{\sqrt[4]{4EIK}} \tag{12}$$

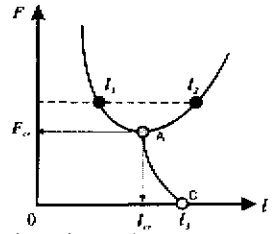

Figure 2 Complete solution of F with induced wavelength l

2.2 Stratum surround by soft matrix

As the stratum is confined by matrix instead of spring, an approximate governing equation can be obtained as (Biot, 1937; Currie *et al.*, 1962):

$$Y''''(X) + \frac{F}{\overline{E}I}Y''(X) + \frac{2\pi\overline{E}_o}{\overline{E}Il}Y(X) = 0 \tag{13}$$

where $\overline{E} = \frac{E}{(1-\nu^2)}$; $\overline{E}_o = \frac{E_o}{(1-\nu^2)}$; E_o = Young's modulus of the matrix; ν = Poisson ratio.

As Eqn. 13 is similar to Eqn. 1, the characteristics of its solution is similar to those described in Section 2.1, except that the term, $\sqrt{4EIK}$, is now replaced by $\frac{3}{2}\sqrt[3]{2\overline{E}I\overline{E}_o^2}$ instead.

The relation of exerted force F and the wavelength can then be determined as (Currie *et al.*, 1962):

$$F = \frac{4\pi^2\overline{E}I}{l^2} + \frac{\overline{E}_o l}{2\pi} \tag{14}$$

Similarly, F_{cr} and l_{cr} can be obtained as:

$$F_{cr} = \frac{3}{2}\sqrt[3]{2\overline{E}I\overline{E}_o^2} \tag{15}$$

$$l_{cr} = 2\pi h \sqrt{\frac{\bar{E}}{6E_s}} \tag{16}$$

where h is the thickness of the layer.

3 NUMERICAL SIMULATION OF BUCKLE FOLDING

To prevent the initial geometric imperfect affecting the yielded buckle fold, the hard layer is set to be flat without initial imperfection. The process to produce buckle fold is as follows: the layer together with the matrix are shortened with an initial shorting strain ε_i, followed by applying moment at one end of the layer to buckle the stratum.

The initial shorten strain ε_i can be expressed in terms of initial shorting length (ΔL) as:

$$\varepsilon_i = \frac{\Delta L}{L} \tag{17}$$

where: L = Length of the layer; A = cross-sectional area of the layer. A dimensionless measure of lateral stress, σ, exerted on the end of strata is defined as:

$$\sigma = \frac{F}{EA} \tag{18}$$

The σ–ε relationship of a layer before and after folding is illustrated by Fig. 3. If the layer is purely shortened without buckling, the σ–ε curve follow a linear segment AB. If the stratum is buckled at C, then it will follow segment CD for the subsequent shortening. This indicates that the buckled stratum (segment ACD) accumulated less strain energy compared to the pure shortening case (segment ACB).

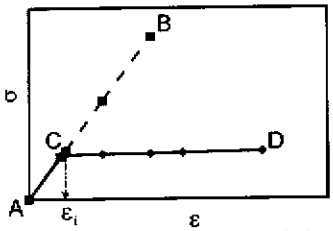

Figure 3 Schematic illustration of the σ–ε relationship of the stratum

When $F < F_{cr}$, the yield fold exhibits decaying nature of its amplitude (Fig. 4) as indicated by Eqn. 8.

Figure 4 Geometry of fold yielded when $F < F_{cr}$

As $F > F_{cr}$, the fold exhibits a "bi-frequency" nature. As shown in Fig. 5, at the commencement of buckling (Fig. 5a), the fold comprises wave of two frequencies. Upon the subsequent shortening of the stratum, the waveform with greater wavelength (l_2) has much greater amplitude than another waveform (l_1) (Fig. 5b), and l_2 hence becomes a dominant wavelength.

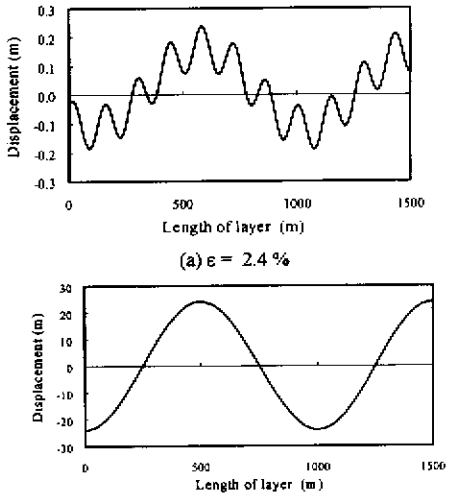

Figure 5 Deformation of stratum when $F > F_{cr}$

The geometry of the fold shown in Fig. 5a is similar to the two-ordered fold observed by geologists. According to Price & Cosgrove (1990), an earlier buckling (with shorter wavelength; second-order fold) increases the effective thickness of the stratum (from a_1 to a_2 shown in Fig.6) and forms a longer wavelength (first-order fold) at a later stage of buckling.

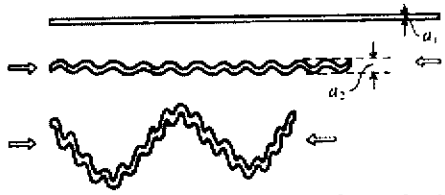

Figure 6 Interpretation to the development of two-ordered fold by Price & Cosgrove (1990)

If the "bi-frequency" nature of fold do exist for $F > F_{cr}$, this simulation result provides another possible mechanism for the underlain mechanism of two-ordered fold. However, the layer may possess viscous behavior, especially under high temperature and high pressure condition; therefore, the impact of viscosity should be accessed before any further interpretation of bi-frequency phenomenon.

The buckle of a multi-layer strata system may induce a poly-harmonic fold. Based on results of

numerical analyses, the development of poly-harmonic fold is as follows:

1 When the stratum is compressed, the middle layer is first buckled with a wavelength as indicated in Fig. 7a;
2 Upon subsequent compression, the adjacent layers, hereafter referred as "boundary layer", are then buckled, which possesses a longer wavelength than that of the middle layer (Fig. 7b);
3 As the amplitude of the folded boundary layers is great enough to affect the middle layer, the middle layer is forced to deflect again according to the waveform of the boundary layers.

This process is identical the interpretation by Ramberg (1964).

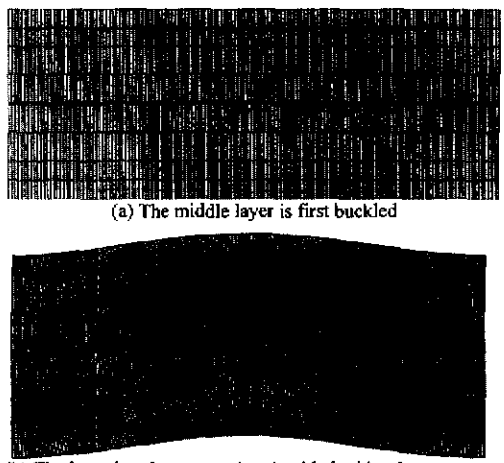

(a) The middle layer is first buckled

(b) The boundary layers are then buckled with a longer wavelength

Figure 7 Development of poly-harmonic fold of multi-layer strata indicated by numerical analysis.

4 CONCLUSIVE REMARKS

An alternative perturbation method is proposed to achieve numerical simulation of folding without introducing the effect of "initial geometry perturbation". The simulation technique allows studying the underlain folding mechanism related to the characteristics of the layer and matrix only, instead of geometry imperfection.

Meanwhile, a complete general solution for a singe, elastic layer embedded in soft matrix is provided such that the solution and the simulation results can be compared and justified. The solution indicates that folding is possible for both $F \geq F_{\sigma}$ and $F < F_{\sigma}$. When $F \geq F_{\sigma}$, the waveform will may comprises of two frequencies. When $F < F_{\sigma}$, decay of wave amplitude occurs.

The mechanism associated with the formation of multi-order fold of a single layer as well as the poly-harmonic fold of a multi-layer system is also explored. For a single layer, the "bi-frequency" nature of the waveform, when $F > F_{\sigma}$, can be a possible cause for multi-order fold.

As revealed by the numerical analysis, the underlain mechanism of poly-harmonic fold of multi-layer can be as follows: high frequency buckle folding along a thinner layer is first initiated at a earlier shortening, followed by buckle of thicker layers at a later shortening. The later folding has a longer wavelength and forces the earlier formed folds to deform with a lower frequency.

REFERENCE

Biot, M.A. 1937. Bending of an infinite beam on an elastic foundation. *J. Applied. Mechanics* **4**: A1-A7.

Biot, M.A. 1961. "Theory of Folding of Stratified Viscoelastic Media and Its Implications in Tectonics and Orogenesis. *Geol. Soc. Am. Bull.* **72**: 1595-1620.

Cobbold, P.R. 1977. Finite-element Analysis of Fold Propagation – a Problematic Application? *Tectonophysics* **38**: 339-353.

Currie, J.B., A.W. Patnode & R.P. Trump 1962. Development of Folds in Sedimentary Strata. *Geol. Soc. Am. Bull.* **73**: 461-472.

Fletcher, R.C. 1977. Folding of a single viscous layer: exact infinitesimal amplitude solution. *Tectonophysics* **39**: 593-606.

Hunt, G.W., H.-B. Mühlhaus & A.I.M. Whiting 1996. Evolution of localized folding for a thin elastic layer in a softening visco-elastic medium. *PAGEOPH* **146(2)**: 229- 252.

Karman, T.V. & M.A. Biot 1940. *Mathematical methods in engineering*, New York :Mcgraw-Hill.

Lan, L. and P. J. Hudleston 1991. Finite-element models of buckle folds in non-linear materials. *Tectonophysics* **199**: 1-12.

Mancktelow, N.S. 1999. Finite-element modeling of single-layer folding in elasto-viscous materials: the effect of initial perturbation geometry. *J. of Structural Geology* **21**: 161-177.

Mühlhaus, H.-B., H. Sakaguchi & B.E. Hobbs 1998. Evolution of three-dimensional folds for a non-Newtonian plate in a viscous medium. *Proc. R. Soc. Lond. A.* **454**: 3121-3143.

Price, N.J. & J.W. Cosgrove 1990. *Analysis of geological structures.* Cambridge: Cambridge Univ. Press.

Ramberg, H. 1964. Selective buckling of composite layers with contrasted rheological properties; a theory for simultaneous formation of several orders of folds. *Tectonophysics* **1**: 307-341.

Zhang, Y., B.E. Hobbs, A. Ord & H.B. Mühlhaus 1996. Computer simulation of single-layer buckling. *J. of Structural Geology* **18 (5)**: 643-655.